Pré-Publicações do Departamento de Matemática
Universidade de Coimbra
Preprint Number 13–42

A 3D MODEL FOR MECHANISTIC CONTROL OF DRUG RELEASE

J.A. FERREIRA, M. GRASSI, E. GUDIÑO AND P. DE OLIVEIRA

Abstract: A 3D mathematical model for sorption/desorption by a cylindrical polymeric matrix with dispersed drug is proposed. The model is based on a system of partial differential equations coupled with boundary conditions over a moving boundary. We assume that the penetrant diffuses into a swelling matrix and causes a deformation which induces a stress driven diffusion and consequently a non-Fickian mass flux. A physically sound non linear dependence between strain and penetrant concentration is considered and introduced in a Boltzmann integral with a kernel computed from a Maxwell-Wiechert model. Numerical simulations show how the mechanistic behavior can have a role in drug delivery design.

Key words: non-Fickian diffusion, viscoelastic behavior, drug delivery, finite difference methods,

Mathematics Subject Classification (2000): 65M06, 65M12, 65M15

1. Introduction

In this paper we study a 3D model of diffusion of a solvent into a cylindrical polymeric matrix containing drug and followed by the drug release. To describe drug release from a polymeric matrix, several models have been proposed [10, 11, 12, 14, 17, 23, 24]. However to the best of our knowledge, the influence of the mechanical properties of a swelling polymer in the sorption of a solvent and in the desorption of drug has not yet been considered in the literature. We propose a model where we combine non-Fickian sorption of the liquid agent, non-Fickian desorption coupled with non-linear dissolution and polymer swelling.

It is well known that the diffusion of a liquid agent into a polymeric sample cannot be completely described by Fick's classical law. The liquid strains the polymeric matrix that while swelling exerts a stress that acts as a barrier to the incoming fluid. To explain these phenomena several authors [2, 4, 5, 10, 20, 21, 22] agree that a modified flux must be considered, that is

$$\frac{\partial C_l}{\partial t} = -div(J_F(C_l) + J_{NF}(\sigma_l)) \ , \tag{1}$$

Received September 25, 2013.

where C_l stands for the concentration of the penetrant, $J_F(C_l) = -(D(C_l)\nabla C_l)$ represents the Fickian part of the flux, $J_{NF}(\sigma_l) = -(D_v(C_l)\nabla\sigma_l)$ represents the non-Fickian part of the flux and σ_l stands for the stress. The functions $D(C_l)$and $D_v(C_l)$ represent respectively the Fickian diffusion coefficient and a viscoelastic diffusion coefficient. Since equation (1) is coupled with a stress evolution equation, the strain ϵ is introduced as a third variable. Many different constitutive relationships between stress and strain have been considered in the literature [2, 4, 3, 5, 15, 16]. In this paper we propose the use of a Boltzmann integral of type

$$\sigma(t) = -\int_0^t E(t-s)\frac{\partial\epsilon}{\partial s}(s)ds \ , \tag{2}$$

where $E(t)$ is the relaxation modulus corresponding to a Maxwell-Wiechert model [1, 18]. We note that the minus sign in (2) means that as the penetrant solvent strains the polymeric matrix, a stress of opposite sign is developed. When (2) is introduced in (1), the strain must be eliminated as a variable. Therefore we consider a non-linear functional relation between strain and concentration

$$\epsilon = f(C_l) \ , \tag{3}$$

where f is established using physical arguments [6], as we will briefly describe in Section 2.

We assume that as the solvent penetrates the polymer the drug is present in two states (dissolved and undissolved) and also that the drug release is controlled by both non-Fickian diffusion and a non-linear dissolution. As the amount of dissolved drug does not induce, locally, any kind of re-arrangement of the polymeric chains, the non-Fickian character of the diffusion equation that describes the drug release is due to solvent uptake.

We track the moving front resulting from the swelling of the polymer by considering a volume conservation equation [23]. As we assume the swelling to be independent in the radial and axial directions we use this volume conservation equation to track separately both of the moving fronts [8].

In Section 2 we establish a mathematical model to describe the absorbtion and drug release. In Section 3 we introduce a volume conservation equation to describe the swelling of the polymeric matrix. In Section 4 an Implicit-Explicit (IMEX) numerical scheme is used to numerically solve the model. In Section 5 some plots are presented to illustrate the behavior of the numerical solutions. Finally in Section 6 some conclusions are addressed.

[18] S. Shaw, J. R. Whiteman, Some partial differential Volterra equation problems arising in viscoelasticity, Proceeding of the Conference on Differential Equations and their Applications, Brno, August 25-29, 1997, ed. R. P. Agarwal, F. Neuman, J.Vosmanský, 183–200, 1998.
[19] Y. Li, T. Tanaka, Effects of shear modulus of polymer gels, in Polymer Gels: fundamental and biomedical applications, DeRossi, D., Kajiwara, K., Osada, Y., Yamauchi, A. eds. Plenum Press, New York, 41–56, 1991.
[20] L.N. Thomas, A.H. Windle, A deformation model for case II diffusion, Polymer, 21: 613–619, 1980.
[21] L.N. Thomas, A.H. Windle, Diffusion mechanics of the system PMMA-methano, Polymer, 22: 627–639, 1981.
[22] L.N. Thomas, A.H. Windle, A theory of case II diffusion, Polymer, 23: 529–542, 1982.
[23] D.E. Pelinovsky, W. Zhao, Multilevel computations of dispersed drug release, Numerical Methods for Partial Differential Equations, DOI: 10.1002/num.21761.
[24] X.Y. Wu, Y. Zhou, Studies of diffusional release of a dispersed solute from polymeric matrices by finite element method, J. Pharm. Sci, 88: 1050–1057, 1999.

J.A. Ferreira
CMUC-Department of Mathematics, University of Coimbra, Apartado 3008, 3001-454 Coimbra, Portugal
E-mail address: ferreira@mat.uc.pt

M. Grassi
Department of Engineering and Architecture, Trieste University, I-34127 Trieste, Italy
E-mail address: mariog@dicamp.univ.trieste.it

E. Gudiño
CMUC-Department of Mathematics, University of Coimbra, Apartado 3008, 3001-454 Coimbra, Portugal
E-mail address: egudino@gmail.com

P. de Oliveira
CMUC-Department of Mathematics, University of Coimbra, Apartado 3008, 3001-454 Coimbra, Portugal
E-mail address: poliveir@mat.uc.pt

to matrices characterized by an increasing polymer concentration. Finally it is worth mentioning that all the parameters of the model can be measured or estimated according to well-known theories.

7. Acknowledgements

This work was partially supported by the Centro de de Matemática da Universidade de Coimbra (CMUC), funded by the European Regional Development Fund through the program COMPETE and by the Portuguese Government through the FCT - Fundação para a Ciência e Tecnologia under the projects PEst-C/MAT/UI0324/2011, UTAustin/MAT/0066/2008 and the scholarship SFR/BD/33703/2009.

References

[1] H.F. Brinson, L.C. Brinson, Polymer Engineering Science and Viscoelasticity, An Introduction, Springer, 2008.
[2] G. Camera-Roda, G.C. Sarti, Mass transport with relaxation in polymers, AIChE Journal, 36: 851–860, 1990.
[3] D.S. Cohen, D.A. Edwards, A mathematical model for a dissolving polymer, AIChE Journal, 41: 2345–2355, 1995.
[4] D.S. Cohen, A. B. White Jr., Sharp fronts due to diffusion and viscoelastic relaxation in polymers, SIAM Journal Applied Mathematics, 51: 472–483, 1991.
[5] D.A. Edwards, Non-Fickian Diffusion in thin polymer films, Journal of Polymer Science, Part B: Polymer Physics Edition, 34: 981–997, 1996.
[6] J.A. Ferreira, M. Grassi, E. Gudino, P. de Oliveira, A new look to non-Fickian diffusion, preprint Universidade de Coimbra , 2013.
[7] P.J. Flory, Thermodynamics of high polymer solutions, J. Chem. Phys., 10:51–61, 1942.
[8] G. Fu, W.O. Soboyejo, Investigation of swellable poly (N-isopropylacrylamide) based hydrogels for drug delivery, Materials Science and Engineering C, 31: 1084–1090, 2011.
[9] H. Fujita, Diffusion in polymer-diluent systems, Fortschr Hochpolym Forsch, 3: 1–47, 1961.
[10] M. Grassi, G. Grassi, Mathematical modeling and controlled drug delivery: matrix systems, Current Drug Delivery, 2: 97–116, 2005.
[11] M. Grassi, G. Grassi, R. Lapasin, I. Colombo, Understanding Drug Release and Absorption Mechanisms: A Physical and Mathematical Approach, CRC Press, 2006.
[12] M. Grassi, S.H. Yuk, S.H. Cho, Modelling of solute transport a temperature-sensitive polymer, J. Membrane. Sci., 152: 241–249, 1999.
[13] R. Lapasin, S. Pricl, Rheology of industrial polysaccharides: Theory and applications, London: Blackie Academic & Professional, 1995.
[14] P.I. Lee, Diffusional release of a solute from a polymeric matrix-approximate analytical solutions. J. Membr. Sci., 7: 255–275, 1980.
[15] Q. Liu, D. De Kee, Modeling of diffusion through polymeric membranes, Rheologica Acta 44: 287–294, 2005.
[16] Q. Liu, X. Wang, D. De Kee, Mass transport through swelling membranes, International Journal of Engineering Science, 43: 1464–1470, 2005.
[17] D.R. Paul, S.K. McSpadden, Diddusional release of a solute from a polymer matrix, J. Membr. Sci., 1: 33–48, 1976.

2. Mathematical model

Let us consider a cylindrical polymeric matrix, with initial solid drug loading C_s^0. As the solvent penetrates the polymeric matrix, solid drug dissolves and dissolved drug diffuses out. The following assumptions are made in the model: (a) swelling is homogeneous and independent in the radial and axial directions; (b) the transport of liquid within the polymer occurs by non-Fickian diffusion; (c) the transport of drug out of the polymer occurs by non-Fickian diffusion associated with solvent uptake and non-linear dissolution; (d) the positions of the polymer swelling front and dissolution front coincide; and (e) a perfect sink condition is maintained for the drug and equilibrium concentrations are maintained for the liquid.

To describe the viscoelastic behavior of the polymer, we consider a generalized Maxwell-Wiechert model [1, 18] with $m+1$ arms in parallel as shown in figure 1. Consequently the relaxation modulus $E(t)$ is represented by

$$E(t) = \sum_{k=1}^{m} E_k e^{\frac{-t}{\tau_k}} + E_0 \ , \tag{4}$$

where the $E_k's$ are the Young modulus of the spring elements, the $\mu_k's$ represent the viscosity, $\tau_k = \frac{\mu_k}{E_k}$ are the relaxation times associated to each of the m Maxwell fluid arms and E_0 stands for the Young modulus of the free spring.

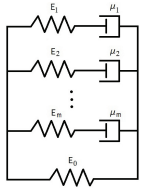

FIGURE 1. Generalized Maxwell-Wiechert model

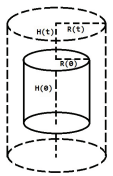

FIGURE 2. Cylindrical domain

Let C_l denote the concentration of the liquid solvent. The functional relation between C_l and the strain ϵ, is defined by

$$f_l(C_l) = \frac{C_l}{\rho_l - C_l} \ . \tag{5}$$

where ρ_l denotes the density of the liquid [6]. Then from (2), (4) and (5) we conclude that the stress associated to solvent uptake and exerted by the

polymer is defined as

$$\sigma_l = -\left(\sum_{k=0}^{m} E_k\right)\nabla f_l + \int_0^t \left(\sum_{k=1}^{m} \frac{E_k}{\tau_k} e^{-\frac{t-s}{\tau_k}}\right)\nabla f_l(s)ds \ . \tag{6}$$

The evolution of solvent penetration, drug diffusion and dissolution are described by the following equations on the domain $\Omega \subset \mathbb{R}^3$ and for $t > 0$,

$$\frac{\partial C_l}{\partial t} = \nabla\cdot(-J_F(C_l) - J_{NF}(\sigma_l)) = \nabla\cdot(D_l(C_l)\nabla C_l + D_v(C_l)\nabla\sigma_l) \ , \tag{7}$$

$$\frac{\partial C_d}{\partial t} = \nabla\cdot(D_d(C_l)\nabla C_d + \upsilon(C_l)C_d) + K_d\left(\frac{C_s - C_d}{C_s}\right)C_l \ , \tag{8}$$

$$\frac{\partial C_s}{\partial t} = -K_d\left(\frac{C_s - C_d}{C_s}\right)C_l \ , \tag{9}$$

where C_d, C_s denote the concentration of dissolved and solid drug respectively, D_l, D_d the diffusion coefficients of the liquid solvent and the dissolved drug respectively, K_d denotes the constant dissolution rate of the drug and υ is defined as

$$\upsilon(C_l) = D_v(C_l)\frac{\nabla\sigma_l}{C_l} \ .$$

Equation (7) states that liquid solvent transport is due to Fickian (J_F) and non-Fickian (J_{NF}) diffusion. At the same time, equation (8) states that the local concentration of dissolved drug depends on Fickian diffusion ($D_d(C_l)\nabla C_d$), convection ($\upsilon(C_l)$) and on solid drug dissolution. While solid drug dissolution can take place provided that $C_l > 0$, the velocity field υ is due to the stress induced by the solvent income. Indeed, we have that $\upsilon = J_{NF}/C_l$.

To establish a functional relation for the viscoelastic diffusion coefficient D_v we follow [6]. We begin by assuming the existence of a stress gradient $\nabla\sigma_l$, that implies the existence of a velocity field ν. Then the non-Fickian flux J_{NF} can be interpreted as a convective field of form

$$J_{NF} = \nu C_l \ . \tag{10}$$

If we compute the velocity field ν using the Hagen-Poiseuille equation, we have

$$\nu = -\frac{R^2}{8\hat{\mu}}\nabla p \ , \tag{11}$$

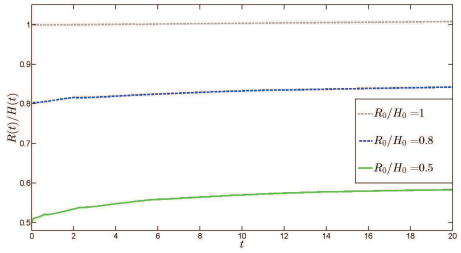

FIGURE 14. $R(t)/H(t)$ as a function of R_0/H_0

flux. To describe this phenomena, we consider a modified flux equation that is the sum of a Fickian flux J_F and a non-Fickian flux J_{NF}. The viscoelastic behavior of the polymer is described by considering a mechanistic system of dampers and springs known as the generalized Maxwell-Wiechert model and by introducing concentration dependent functional relations for the strain and the viscoelastic diffusion coefficient. For the drug release, as we assume that the drug is present in two states dissolved and undissolved, the process is described by Fickian diffusion associated to solvent uptake coupled with non-linear dissolution. To describe the swelling of the polymeric cylinder we consider a volume conservation equation to track the movement of the fronts in both radial and axial directions. To solve the initial-boundary value problem associated to the system of equations we use an Implicit-Explicit (IMEX) method to obtain numerical solutions. We exhibit several plots to illustrate the behavior of the solutions and the influence that the parameters associated to the model have over the drug release.

The great advantage of the proposed model consists in the possibility of easily and directly incorporating experimental rheological information about polymer-solvent matrix system (knowledge of E_k and μ_k). Indeed, once the mechanical spectrum referring to a particular polymer-solvent matrix is experimentally determined by rheological tests (frequency sweep), the Maxwell-Wiechert model (also called generalized Maxwell model by rheologists) can be fitted to experimental data for the determination of E_k and μ_k [13]. Of course, our model could be also implemented considering the dependence of E_k and μ_k on local solvent concentration. Again, this information can be experimentally deduced by determining the mechanical spectrum referring

perfect sink condition is assumed and the mass of drug released decreases as the swelling increases.

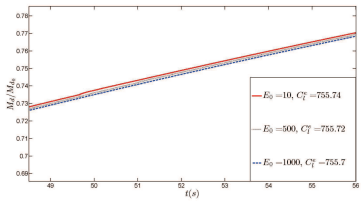

FIGURE 10. Mass of drug released, M_d/M_{d_0} as a function of E_0 with $L(t) = L_0$

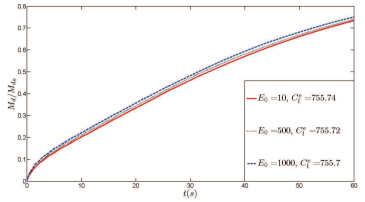

FIGURE 11. Mass of drug released, M_d/M_{d_0} as a function of E_0

In Figures 12 and 13 we show plots of M_s/M_∞ and M_d/M_{d_0} respectively as a function of μ_1. Figure 12 shows that M_s/M_∞ is a decreasing function of μ_1 and Figure 13 that M_d/M_{d_0} is an increasing function of μ_1. In Figure 12 we did a a $5th$ degree polynomial fitting in order to avoid the jumps that appear as a consequence of the moving of the boundary.

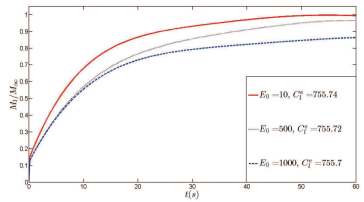

FIGURE 12. Mass of solvent, M_s/M_∞ as a function of the viscosity μ_1

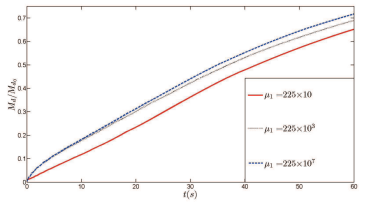

FIGURE 13. Mass of drug released, M_d/M_{d_0} as a function of the viscosity μ_1

Finally in Figure 14 we plotted $R(t)/H(t)$ for different initial values of R_0/H_0. As proved by Tanaka in [19], we observe that upon swelling $R(t)/H(t)$ is constant and approximately equal to R_0/H_0.

6. Conclusions

In this paper a 3D mathematical model to describe the drug release from a cylindrical polymeric matrix is presented. We assume that a solvent diffuses into the matrix creating a stress driven diffusion, thus a non-Fickian mass

where R stands for the radius of a virtual cross section of the polymeric sample available for the convective flux, p is the pressure drop and $\hat{\mu}$ represents the viscosity of a polymer-solvent solution characterized by a liquid (or solvent) concentration equal to C_l (local solvent concentration). Thus from (10) and (11) and identifying the pressure p with the viscoelastic stress σ_l, we conclude that

$$D_v(C_l) = \frac{R^2 C_l}{8\hat{\mu}} \ . \tag{12}$$

Let m_l and V_l represent the mass and volume of the solvent respectively. If ρ_l represents its density, then $m_l = \rho_l V_l$ and $C_l = \frac{m_l}{V_0+V_l}$, where V_0 is the volume of the polymeric matrix in the dry state. We conclude then that

$$V_l = \frac{C_l}{\rho_l - C_l} V_0 \ ,$$

and as $V_0 = \Delta x_0 S$, we have

$$\frac{V_l}{\Delta x_0} = \frac{C_l}{\rho_l - C_l} S \ . \tag{13}$$

The first member in (13) can be interpreted as a virtual cross section S_v available for convective flow. As $S_v = \pi R^2$ and $S = \pi R_0^2$ where R_0 is the radius of the dry sample, we deduce the form of the viscoelastic coefficient D_v,

$$D_v(C_l) = \frac{R_0^2 C_l^2}{8\hat{\mu}(\rho_l - C_l)} \ . \tag{14}$$

A Fujita-type [9] exponential dependence for $D_l(C_l)$ and $D_d(C_l)$ is assumed with

$$D_l(C_l) = D_{eql} exp(-\beta_l(1 - \frac{C_l}{C_l^e})) \ , \tag{15}$$

$$D_d(C_l) = D_{eqd} exp(-\beta_d(1 - \frac{C_l}{C_l^e})) \ , \tag{16}$$

where D_{eql}, D_{eqd} denote respectively the diffusion coefficients of the liquid solvent and the dissolved drug in the fully swollen sample and β_l, β_d dimensionless positive constants.

We consider a cylindrical domain $\Omega \subset \mathbb{R}^3$ with initial radius R_0 and height H_0 (Figure 2). Due to the symmetry in θ direction, the three dimensional

problem is reduced to a two dimensional case. Therefore equations (7)-(9) can be rewritten in cylindrical coordinates as

$$\frac{\partial C_l}{\partial t} = \frac{1}{r}\frac{\partial}{\partial r}\left(rD_l(C_l)\frac{\partial C_l}{\partial r} + rD_v(C_l)\frac{\partial \sigma_l}{\partial r}\right) + \frac{\partial}{\partial z}\left(D_l(C_l)\frac{\partial C_l}{\partial z} + D_v(C_l)\frac{\partial \sigma_l}{\partial z}\right) , \tag{17}$$

$$\frac{\partial C_d}{\partial t} = \frac{1}{r}\frac{\partial}{\partial r}\left(rD_d(C_l)\frac{\partial C_d}{\partial r} + r\upsilon(C_l)C_d\right) + \frac{\partial}{\partial z}\left(D_d(C_l)\frac{\partial C_d}{\partial z} + \upsilon(C_l)C_d\right) + K_d\left(\frac{C_s - C_d}{C_s}\right)C_l , \tag{18}$$

$$\frac{\partial C_s}{\partial t} = -K_d\left(\frac{C_s - C_d}{C_s}\right)C_l , \tag{19}$$

where $0 < r < R(t)$, $0 < z < H(t)$ and $t > 0$. Equations (17)-(19) are completed with initial conditions

$$C_l = C_l^0,\ C_d = 0,\ C_s = C_s^0 \ :\ \text{for } t = 0,\ 0 \le r \le R_0,\ 0 \le z \le H_0 , \tag{20}$$

where $C_l^0,\ C_s^0 \in \mathbb{R}$ are positive constants. At the cylinder surface the boundary conditions are

$$C_l = C_l^e,\ C_d = 0 \ :\ \begin{array}{l}\text{for } t > 0,\ r = R(t),\ 0 \le z \le H(t) \\ \text{and}\ \ z = H(t),\ 0 \le r \le R(t) ,\end{array} \tag{21}$$

where $C_l^e \in \mathbb{R}$ is a positive constant representing the concentration of the liquid agent in the exterior of the cylinder. Symmetry conditions are applied at the center of the matrix, hence we also have that

$$\begin{array}{l}\dfrac{\partial C_l}{\partial z} = \dfrac{\partial C_d}{\partial z} = 0 \ :\ \text{for } t > 0,\ r = 0,\ 0 \le z \le H(t) \\ \dfrac{\partial C_l}{\partial r} = \dfrac{\partial C_d}{\partial r} = 0 \ :\ \text{for } t > 0,\ z = 0,\ 0 \le r \le R(t) .\end{array} \tag{22}$$

3. Tracking of the swelling fronts

In order to track the moving fronts due to swelling, we consider the following conservation equation, where the total volume of the matrix is the sum

In Figures 8 and 9 we present the dimensionless swelling fronts as functions of the parameter E_0 and its corresponding C_l^e. In both cases we observe that the fronts are decreasing functions of E_0. We note that this behavior is physically sound, since an increase in E_0 corresponds to an increase in the resistance of the polymer to swelling.

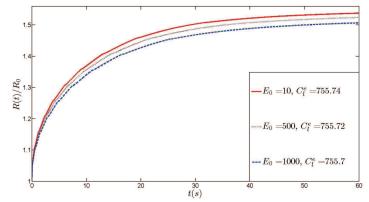

FIGURE 8. Radial swelling, $R(t)/R_0$ as a function of E_0

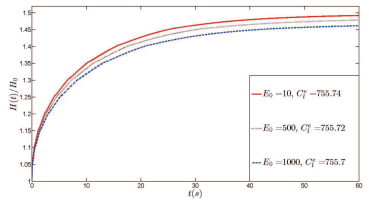

FIGURE 9. Axial swelling, $H(t)/H_0$ as a function of E_0

By $M_d/M_{d_0}(t)$, where M_d is the total mass of drug released at time t and M_{d_0} is the initial mass loaded in the polymeric matrix, we represent the dimensionless total mass of drug released at time t defined as

$$M_d/M_{d_0}(t) = 1 - \frac{2}{R_0^2 H_0 C_s^0}\int_0^{H(t)}\int_0^{R(t)} r\left(C_s(r,z,t) + C_d(r,z,t)\right)dr\,dz . \tag{40}$$

and by $M_s/M_\infty(t)$ the mass of the liquid solvent inside of the matrix at time t, defined as

$$M_s/M_\infty(t) = \frac{2}{R_{eq}^2 H_{eq} C_l^e}\int_0^{H(t)}\int_0^{R(t)} rC_l(r,z,t)dr\ dz , \tag{41}$$

where R_{eq} and H_{eq} are the values of $R(t)$ and $H(t)$ at equilibrium, respectively.

In order the study the effects of swelling in drug release we plotted M_d/M_{d_0} as a function of E_0 in Figures 10 and 11. In Figure 10 we assume that the polymer does not swell and in Figure 11 a moving boundary due to swelling is considered. When we say that no swelling is present we mean that $L(t) = L_0$ for all t. We observe in Figure 10 that M_d/M_{d_0} is a decreasing function of E_0. Conversely in Figure 11 we observe that M_d/M_{d_0} is an increasing function of E_0. As shown in Figures 8 and 9, an E_0 decrease implies a swelling increase and, therefore, the dissolved drug has to travel a larger distance to the moving front. Consequently, less dissolved drug accumulates at the front where the

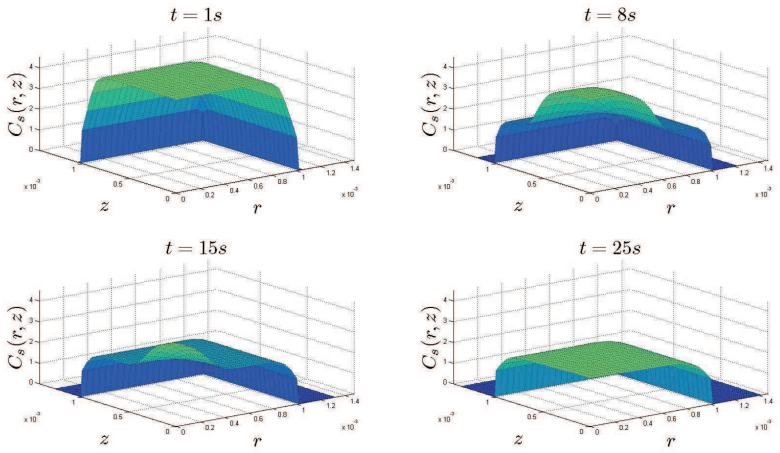

FIGURE 5. Concentration of undissolved drug C_s, for different t

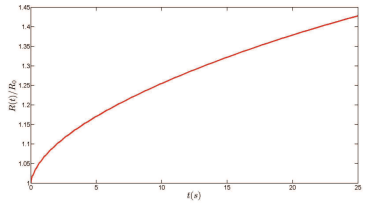

FIGURE 6. Swelling in the radial direction

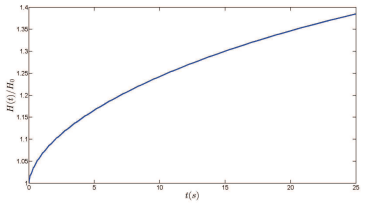

FIGURE 7. Swelling in the axial direction

can be computed with the formula

$$\rho_x = \frac{E_0}{3R_gT} \ , \tag{38}$$

where R_g is the universal gas constant and T the absolute temperature. Assuming that $\chi = 0.6$, $T = 298.15\ K$ and $V_1 = 18.064 \times 10^{-6}\ m^3/mol$, then once E_0 is fixed, ϕ_p can be calculated with (37) and the corresponding C_l^e can be obtained from

$$C_l = \rho_l(1 - \phi_p) \ . \tag{39}$$

of water, dissolved and undissolved drug volumes. We have

$$\begin{aligned} &\pi R^2(t)H(t) \\ &= \int_0^{H(t)} \int_0^{R(t)} 2\pi r \left[\frac{1}{\rho_l} C_l(r,z,t) + \frac{1}{\rho_d}\left(C_d(r,z,t) + C_s(r,z,t)\right)\right] dr\ dz \\ &+ \frac{m_0}{\rho_p} \ , \end{aligned} \tag{23}$$

where ρ_p and ρ_d denote the density of the polymer and the drug respectively, m_0 represent the initial mass of the dry polymeric matrix.

Since we assume the swelling to be independent in the two directions, by taking time derivatives in (23), the moving fronts in the radial and axial direction can be separately tracked.

To track the moving front in the radial direction we begin by fixing $H(t) = H$ and taking time derivative in (23) to obtain

$$\begin{aligned} &R(t)H\frac{\partial R(t)}{\partial t} \\ &= \int_0^{H} \int_0^{R(t)} r \left[\frac{1}{\rho_l} \frac{\partial C_l}{\partial t}(r,z,t) + \frac{1}{\rho_d}\frac{\partial}{\partial t}\left(C_d(r,z,t) + C_s(r,z,t)\right)\right] dr\ dz \\ &+ \int_0^{H} R(t)\frac{\partial R(t)}{\partial t}\left(\frac{C_l^e}{\rho_l} + \frac{C_s|_{R(t)}}{\rho_d}\right) dz \ . \end{aligned} \tag{24}$$

As we have that

$$\begin{aligned} &\int_0^{H} \int_0^{R(t)} \frac{r}{\rho_l}\frac{\partial C_l}{\partial t}(r,z,t) dr\ dz \\ &= \int_0^{H} \frac{R(t)}{\rho_l}\left(D_l(C_l(R(t),z,t))\frac{\partial C_l}{\partial r}(R(t),z,t)\right. \\ &\left. + D_v(C_l(R(t),z,t))\frac{\partial \sigma_l}{\partial r}(R(t),z,t)\right) \end{aligned} \tag{25}$$

and

$$\begin{aligned} &\int_0^{H} \int_0^{R(t)} r\frac{1}{\rho_d}\frac{\partial}{\partial t}\left(C_d(r,z,t) + C_s(r,z,t)\right) dr\ dz \\ &= \int_0^{H} \frac{R(t)}{\rho_d} D_d(C_l(R(t),z,t))\frac{\partial C_d}{\partial r}(R(t),z,t) dz \ , \end{aligned} \tag{26}$$

it follows from (24)-(26) that

$$\left(1-\frac{C_l^e}{\rho_l}-\frac{C_s|_{R(t)}}{\rho_d}\right)H\frac{\partial R(t)}{\partial t}$$
$$=\int_0^H\left[\frac{1}{\rho_l}\left(D_l(C_l^e)\frac{\partial C_l}{\partial r}(R(t),z,t)+D_v(C_l^e)\frac{\partial \sigma_l}{\partial r}(R(t),z,t)\right)+\frac{1}{\rho_d}\right.$$
$$\left.+D_d(C_l^e)\frac{\partial C_d}{\partial r}(R(t),z,t)\right]dz\ . \tag{27}$$

To track the moving front in the axial direction, we fix $R(t)=R$ and proceeding as before we deduce

$$\left(1-\frac{C_l^e}{\rho_l}-\frac{C_s|_{H(t)}}{\rho_d}\right)R^2\frac{\partial H(t)}{\partial t}$$
$$=2\int_0^R\left[\frac{1}{\rho_l}\left(D_l(C_l^e)\frac{\partial C_l}{\partial z}(r,H(t),t)+D_v(C_l^e)\frac{\partial \sigma_l}{\partial z}(r,H(t),t)\right)\right.$$
$$\left.+\frac{1}{\rho_d}D_d(C_l^e)\frac{\partial C_d}{\partial z}(r,H(t),t)\right]r\ dr\ . \tag{28}$$

We note that if no mechanistic effects are taken into account and the drug is considered to exist only in the dissolved state then (27) and (28) reduce to the moving boundary conditions in [8].

4. Numerical scheme

In this section we propose a coupled Implicit-Explicit (IMEX) method to solve the initial-boundary value problem (17)-(22) and (27), (28).

In $[0,T]$ we consider a grid $P=\{t_n, n=0,1,...,M\}$ with $t_0=0$, $t_M=T$ and $t_n-t_{n-1}=\Delta t$. We denote by D_{-t} the usual backward finite difference operator with respect to the time variable.

As the spatial boundary is changing in time, we consider in the initial interval $[0,R_0]$ a uniform grid $I(t_0)=\{r_i,\ i=0,1,..,N(t_0)\}$ with $r_0=0$, $r_{N(t_0)}=R_0$ and $r_i-r_{i-1}=\Delta r$. Then in each interval $[0,R(t_n)]$ we consider a non-uniform grid $I(t_n)=\{r_i,\ i=0,1,..,N(t_n)\}$ with $r_0=0$, $r_{N(t_n)}=R(t_n)$ and $r_i-r_{i-1}=\Delta r_i$. We denote by D_{-r} and D_r the usual backward and forward finite difference operator with respect to the space variable r.

Analogously in the initial interval $[0,H_0]$ we consider a uniform grid $J(t_0)=\{z_j,\ j=0,1,..,N(t_0)\}$ with $z_0=0$, $z_{K(t_0)}=H_0$ and $z_j-z_{j-1}=\Delta z$. Then

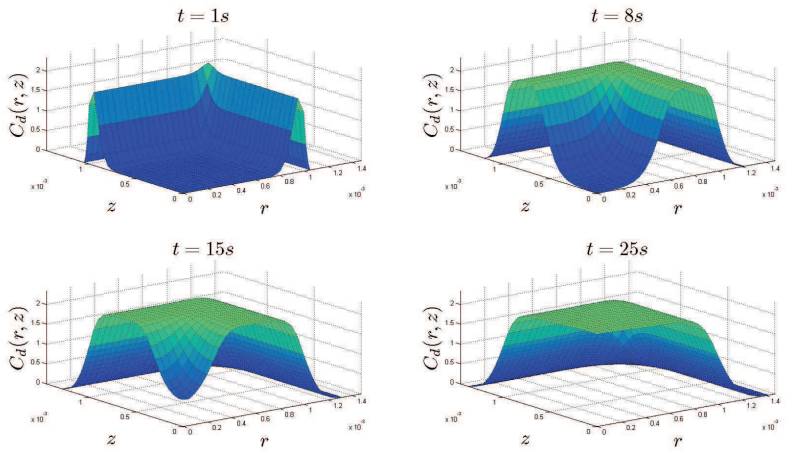

FIGURE 4. Concentration of dissolved drug C_d, for different t

In Figure 5 we show plots of the concentration of solid drug at $t=1s$, $t=8s$, $t=15s$ and $t=25s$. We observe that as the concentration of dissolved drug increases, the concentration of solid drug decreases smoothly towards the moving fronts. On the contrary to what is observed in the plots of dissolved drug, the regions of highest solid drug concentration correspond to regions of lowest liquid agent concentration.

In Figures 6 and 7 we plotted the movement in time of the dimensionless swelling fronts in both axial and radial directions. We observe that in both cases, the initial uptake of the solvent produces an initial rapid growth of the swelling followed by an equilibrium state of the fronts.

According to Flory theory [7] there is a link between E_0 and C_l^e, more precisely, at equilibrium we have

$$ln(1-\phi_p)+\phi_p+\chi\phi_p^2+\rho_x V_1\left(\phi_p^{\frac{1}{3}}-0.5\phi_p\right)=0\ , \tag{37}$$

where ϕ_p represent the polymer volume fraction, V_1 the solvent molar volume, ρ_x is the crosslink density and χ is the Flory interaction parameter. As ρ_x

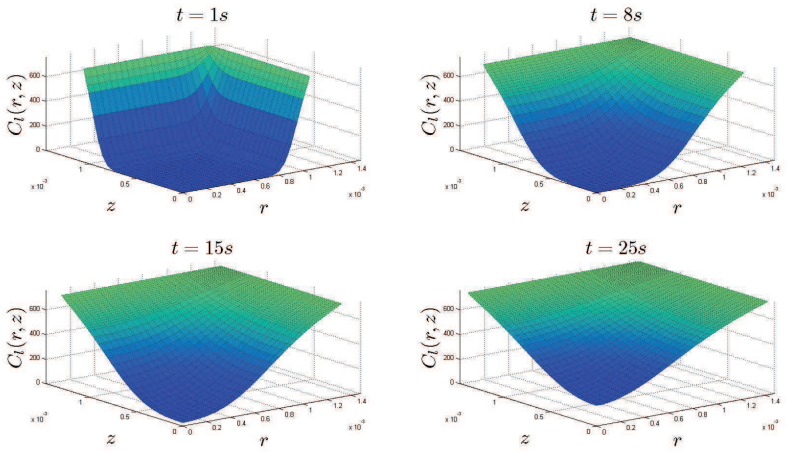

FIGURE 3. Concentration of solvent C_l, for different t

inner part of the cylinder where symmetry conditions (22) were considered. The outermost part of the plots correspond to the expansion fronts where a perfect sink condition is assumed. We observe that regions where the concentration of the liquid solvent is high, correspond to regions where the concentration of dissolved drug is also high.

in each one of the intervals $[0, H(t_n)]$ for $n = 0, 1, ..., M$, we consider a non-uniform grid $J(t_n) = \{z_j,\ j = 0, 1, .., K(t_n)\}$ with $z_0 = 0$, $z_{K(t_n)} = H(t_n)$ and $z_j - z_{j-1} = \Delta z_j$. We denote by D_{-z} and D_z the usual backward and forward finite difference operator with respect to the space variable z.

Let M_{h_r} and M_{h_z} be defined as

$$\begin{aligned} M_{h_r}u_h(r_i, z_j) &= \frac{1}{2}(u_h(r_{i-1}, z_j) + u_h(r_i, z_j)) \ , \\ M_{h_z}u_h(r_i, z_j) &= \frac{1}{2}(u_h(r_i, z_{j-1}) + u_h(r_i, z_j)) \ , \end{aligned}$$

then we introduce the following notations

$$\begin{aligned} IM_{l,r}(r_i, z_j, t_n) &= D_l(M_{h_r}C^{n-1}_{l_h}(r_i, z_j))D_{-r}C^n_{l_h}(r_i, z_j) \ , \\ IM_{l,z}(r_i, z_j, t_n) &= D_l(M_{h_z}C^{n-1}_{l_h}(r_i, z_j))D_{-z}C^n_{l_h}(r_i, z_j) \ , \\ EX_{l,r}(r_i, z_j, t_{n-1}) &= D_v(M_{h_r}C^{n-1}_{l_h}(r_i, z_j))D_{-r}\sigma^{n-1}_{l_h}(r_i, z_j) \ , \\ EX_{l,z}(r_i, z_j, t_{n-1}) &= D_v(M_{h_z}C^{n-1}_{l_h}(r_i, z_j))D_{-z}\sigma^{n-1}_{l_h}(r_i, z_j) \ . \end{aligned}$$

and

$$\begin{aligned} IM_{d,r}(r_i, z_j, t_n) &= D_d(M_{h_r}C^n_{l_h}(r_i, z_j))D_{-r}C^n_{d_h}(r_i, z_j) \ , \\ IM_{d,z}(r_i, z_j, t_n) &= D_d(M_{h_z}C^n_{l_h}(r_i, z_j))D_{-z}C^n_{d_h}(r_i, z_j) \ , \\ EX_{d,r}(r_i, z_j, t_{n-1}) &= D_v(M_{h_r}C^n_{l_h}(r_i, z_j))\frac{M_{h_r}C^n_{d_h}(r_i, z_j)}{M_{h_r}C^n_{l_h}(r_i, z_j)}D_{-r}\sigma_{l_h}(C^n_{l_h}(r_i, z_j)) \ , \\ EX_{d,z}(r_i, z_j, t_{n-1}) &= D_v(M_{h_z}C^n_{l_h}(r_i, z_j))\frac{M_{h_z}C^n_{d_h}(r_i, z_j)}{M_{h_z}C^n_{l_h}(r_i, z_j)}D_{-z}\sigma_{l_h}(C^n_{l_h}(r_i, z_j)) \ , \end{aligned}$$

where we have used IM and EX to underline the implicit and the explicit character of the discretization respectively.

The IMEX method for (17)-(19) is defined by

$$\begin{aligned} D_{-t}C^n_{l_h}(r_i,z_j) &= \frac{1}{r_i}D_r\left((M_{h_r}r_i)IM_{l,r}(r_i,z_j,t_n)+(M_{h_r}r_i)EX_{l,r}(r_i,z_j,t_{n-1})\right) \\ &\quad +D_z\left(IM_{l,z}(r_i,z_j,t_n)+EX_{l,z}(r_i,z_j,t_{n-1})\right)\ , \qquad (29) \\ D_{-t}C^n_{d_h}(r_i,z_j) &= \frac{1}{r_i}D_r\left((M_{h_r}r_i)IM_{d,r}(r_i,z_j,t_n)+(M_{h_r}r_i)EX_{d,r}(r_i,z_j,t_{n-1})\right) \\ &\quad +D_z\left(IM_{d,z}(r_i,z_j,t_n)+EX_{d,z}(r_i,z_j,t_{n-1})\right) \\ &\quad +K_d\left(\frac{C^{n-1}_{s_h}(r_i,z_j)-C^{n-1}_{d_h}(r_i,z_j)}{C^{n-1}_{s_h}(r_i,z_j)}\right)C^n_{l_h}(r_i,z_j)\ , \qquad (30) \\ D_{-t}C^n_{s_h}(r_i,z_j) &= -K_d\left(\frac{C^{n-1}_{s_h}(r_i,z_j)-C^n_{d_h}(r_i,z_j)}{C^{n-1}_{s_h}(r_i,z_j)}\right)C^n_{l_h}(r_i,z_j)\ , \qquad (31) \end{aligned}$$

with initial conditions

$$C^0_{l_h}=C^0_l,\ C^0_{d_h}=0,\ C_{s_h}=C^0_s\ :\ \text{for } t=0,\ 0\le r_i\le R_0,\ 0\le z_j\le H_0\ , \qquad (32)$$

boundary conditions on the cylinder surface

$$\begin{aligned} C_{l_h}=C^e_l,\ C_{d_h}=0\quad &:\quad \text{for } n>0,\ r_i=R(t_n),\ 0\le z_j\le H(t_n) \\ &\quad \text{and}\ \ z_j=H(t_n),\ 0\le r_i\le R(t_n)\ , \qquad (33) \end{aligned}$$

and boundary conditions at the symmetric axes

$$\begin{aligned} D_{-z}C_{l_h}=D_{-z}C_{d_h}=0\quad &:\quad \text{for } n>0,\ r_i=0,\ 0\le z_j\le H(t_n) \\ D_{-r}C_{l_h}=D_{-r}C_{d_h}=0\quad &:\quad \text{for } n>0,\ z_j=0,\ 0\le r_i\le R(t_n)\ . \qquad (34) \end{aligned}$$

The moving front defined by (27) and (28) is tracked with the following equations

$$\begin{aligned} &\left(1-\frac{C^e_l}{\rho_l}-\frac{C_s|_{R(t_n)}}{\rho_d}\right)H(t_n)D_{-t}R(t_{n+1}) \\ &=\Delta z\sum_{j=1}^{K(t_n)}\frac{1}{\rho_l}\left(D_l(C^e_l)D_{-r}C^n_{l_h}(R(t_n),z_j)+D_v(C^e_l)D_{-r}\sigma^n_{l_h}(R(t_n),z_j)\right) \\ &+\frac{1}{\rho_d}D_d(C^e_l)D_{-r}C^n_{d_h}(R(t_n),z_j\ , \qquad (35) \end{aligned}$$

and

$$\begin{aligned} &\left(1-\frac{C^e_l}{\rho_l}-\frac{C_s|_{H(t_n)}}{\rho_d}\right)R^2(t_n)D_{-t}H(t_{n+1}) \\ &=2\Delta r\sum_{i=1}^{N(t_n)}\frac{r_i}{\rho_l}\left(D_l(C^e_l)D_{-r}C^n_{l_h}(r_i,H(t_n))+D_v(C^e_l)D_{-r}\sigma^n_{l_h}(r_i,H(t_n))\right) \\ &+\frac{r_i}{\rho_d}D_d(C^e_l)D_{-r}C^n_{d_h}(r_i,H(t_n))\ . \qquad (36) \end{aligned}$$

We compute the concentration profiles at time step t_n using the known concentration profiles at t_{n-1} with boundary conditions (33) and (34). Then we use (35) and (36) to obtain the new front position for the next time step.

5. Numerical Results

In what follows we exhibit some numerical results for the initial-boundary value problem (17)-(22) and (27), (28) using the method (29)-(36). In (4) we consider $m=1$, that is a Maxwell fluid arm in parallel with a free spring. The following values for the parameters have been considered,

$$\begin{aligned} R_0 &= 1\times10^{-3}\ m,\ \Delta r_{max}=5\times10^{-5}\ m,\ H_0=1\times10^{-3}\ m, \\ \Delta z_{max} &= 5\times10^{-5}\ m,\ D_{eq_l}=3.74\times10^{-9}\ m^2/s,\ D_{eq_d}=2.72\times10^{-10}\ m^2/s, \\ \beta_l &= 0.8,\ \beta_d=0.5,\ \hat{\mu}=20\times10^5\ Pas,\ \rho_l=1000\ kg/m^3, \\ \rho_p &= 1175\ kg/m^3,\ \rho_d=1400\ kg/m^3,\ E_1=9\times10^3\ Pa, \\ E_0 &= 1\times10^3\ Pa,\ \mu_1=225\times10^4\ Pas,\ C^e_l=755\ Kg/m^3, \\ C^0_l &= 0\ Kg/m^3,\ C^0_s=4.5\ Kg/m^3,\ K_d=1\times10^{-2}\ s^{-1}\ \text{and}\ \Delta t=0.01\ s. \end{aligned}$$

In Figure 3 we plotted the behavior of the concentration of the liquid solvent as it diffuses into the polymeric cylinder at $t=1s$, $t=8s$, $t=15s$ and $t=25s$. A quarter of the cylinder cross section was modeled due to symmetries. The axes z and r correspond to the inner part of the cylinder where symmetry conditions (22) were considered. The outer parts correspond to the expansion fronts where the constant source of concentration C^e_l is assumed. We observe a smooth solution that develops from low levels of concentration to high levels of concentration as expected, since the liquid penetration occurs from the outermost regions of the plot toward the axes.

In Figure 4 we present plots of the concentration of dissolved drug at $t=1s$, $t=8s$, $t=15s$ and $t=25s$. As before, the axes z and r correspond to the